

# Neuroscience and accelerator mass spectrometry

Magnus Palmblad, Bruce A. Buchholz, Darren J. Hillegonds and John S. Vogel\*

Center for Accelerator Mass Spectrometry, Lawrence Livermore National Laboratory, Livermore, California 94551

Received 31 March 2004; Accepted 29 July 2004

Accelerator mass spectrometry (AMS) is a mass spectrometric method for quantifying rare isotopes. It has had a great impact in geochronology and archaeology and is now being applied in biomedicine. AMS measures radioisotopes such as  $^3\text{H}$ ,  $^{14}\text{C}$ ,  $^{26}\text{Al}$ ,  $^{36}\text{Cl}$  and  $^{41}\text{Ca}$ , with zepto- or attomole sensitivity and high precision and throughput, allowing safe human pharmacokinetic studies involving microgram doses, agents having low bioavailability or toxicology studies where administered doses must be kept low ( $<1\ \mu\text{g kg}^{-1}$ ). It is used to study long-term pharmacokinetics, to identify biomolecular interactions, to determine chronic and low-dose effects or molecular targets of neurotoxic substances, to quantify transport across the blood–brain barrier and to resolve molecular turnover rates in the human brain on the time-scale of decades. We review here how AMS is applied in neurotoxicology and neuroscience. Copyright © 2005 John Wiley & Sons, Ltd.

**KEYWORDS:** accelerator mass spectrometry; carbon-14; radiocarbon; diisopropyl fluorophosphate; Alzheimer's disease

## INTRODUCTION

The use of radioisotopes has a long history in biochemistry.<sup>1,2</sup> Accelerator mass spectrometry (AMS) is an exquisitely sensitive mass spectrometric method for measuring rare isotopes, especially radioisotopes. The technique is primarily applied in geochronology to date samples using long-lived radioisotopes that are detected independent of their decay products or half-life. In the last decade, AMS has also emerged as a sensitive tool for bioanalytical tracing, quantitating isotope concentrations to parts per quadrillion (1 in  $10^{15}$ ).<sup>3</sup> This translates to zepto- to attomoles of the isotopically labeled compounds in micro- to milligram samples. Even smaller samples, down to single eukaryotic cells,<sup>4</sup> are experimentally feasible with the addition of a well-characterized carrier or unlabeled cells. In conventional mass spectrometry, isotopic concentrations below 1 part in  $10^7$  cannot be reliably measured owing to interferences from atomic or molecular isobars. AMS has superior concentration and mass detection limits to those of liquid scintillation counting.<sup>5</sup> Moreover, whereas there are many mass spectrometric techniques for relative quantitation, AMS is absolutely quantitative.

A significant number of rare isotopes are measurable by AMS, such as  $^3\text{H}$ ,  $^{14}\text{C}$ ,  $^{26}\text{Al}$ ,  $^{36}\text{Cl}$ ,  $^{41}\text{Ca}$  and numerous isotopes of heavier elements.<sup>6</sup> This paper briefly reviews how  $^{14}\text{C}$  AMS is applied to biomedical problems in general and neuroscience in particular. It will focus on the analyses of  $^{14}\text{C}$

in biological tissues and the use of  $^{14}\text{C}$  labeling since it is most mature of the AMS isotopes and measurement is routine. AMS is also applied in neuroscience for  $^{26}\text{Al}$  analysis in brain, recently reviewed by Yokel and McNamara.<sup>7</sup> Although  $^3\text{H}$  labeling is well established and chlorine and calcium are of great interest, AMS has not yet been applied in neuroscience using these isotopes.

## CARBON-14 ACCELERATOR MASS SPECTROMETRY

Biological samples containing 0.2–5 mg of C in almost any shape, form and composition are placed in quartz tubes with excess copper oxide (CuO), evacuated, sealed and combusted to  $\text{CO}_2$ . The  $\text{CO}_2$  is then reduced to solid carbon, e.g. fullerene or graphite, using a cobalt or iron catalyst.<sup>8–10</sup> This process is independent of the chemical nature of the sample and eliminates interference or suppression from other sample components. However, any information on the chemical nature of the  $^{14}\text{C}$ -containing species is lost in this step and must be obtained prior to combustion to  $\text{CO}_2$ . When studying the metabolism of a labeled molecule or using ambient  $^{14}\text{C}$  or metabolic labeling, this information may have to be recovered by other means, e.g. though specific extraction, separation,<sup>11,12</sup> affinity capture<sup>13</sup> or addition of unlabeled standard(s) followed by an analytical method for chemical identification (e.g. mass spectrometry or nuclear magnetic resonance). AMS is an isotope ratio mass spectrometric technique where  $^{14}\text{C}/^{13}\text{C}$  ratios of unknowns are normalized to measurements of identically prepared standards of known isotope concentration.<sup>4</sup> Like mass spectrometric methods for relative quantitation based on stable-isotope labeling or metabolic incorporation,<sup>14,15</sup> absolute efficiency need not be determined.

\*Correspondence to: John S. Vogel, Center for Accelerator Mass Spectrometry, Lawrence Livermore National Laboratory, Livermore, California 94551, USA. E-mail: vogel@llnl.gov  
Contract/grant sponsor: LLNL; Contract/grant number: LDRD 01-ERI-006.  
Contract/grant sponsor: US Department of Energy; Contract/grant number: W-7405-ENG-48.

The carbon from the reduced sample is pounded into cylindrical target cathodes, which are mounted in a 64-sample wheel and placed inside a cesium sputter ion source. Atomic Cs vapor is produced from a heated cesium reservoir and sprayed on to a heated ionizer surface, producing  $\text{Cs}^+$  ions that are accelerated towards the target held at  $-8$  kV. The  $\text{Cs}^+$  ions sputter carbon atoms and ions from the target that are ionized to  $\text{C}^-$  ions as they pass through a condensed cesium layer on the cathode. Negative ions at  $m/z$  13 ( $^{13}\text{C}^-$ ) and 14 ( $^{14}\text{C}^-$ ) are pulsed through an injection magnet into a tandem electrostatic van der Graaff accelerator (Fig. 1; see also Ognibene *et al.*<sup>16</sup>). Negative  $\text{C}^-$  ions are accelerated towards the high-voltage terminal ( $+518$  kV) in the center of the accelerator where they are converted to positive ions,  $\text{C}^+$  being the most abundant, in an argon gas electron stripper (Fig. 1). The positive ions are repelled toward the high-energy exit of the accelerator held at  $0$  V.  $^{13}\text{C}^+$  and  $^{14}\text{C}^+$  ions are separated by momentum using a high-energy analyzing magnet (Fig. 1). The beam currents of the abundant stable isotopes  $^{12}\text{C}$  and  $^{13}\text{C}$  are measured in Faraday cups. The  $^{12}\text{C}$  cup is positioned after the injection magnet and before the accelerator whereas  $^{13}\text{C}$  cup is positioned between the analyzing magnet and the  $90^\circ$  electrostatic spherical analyzer (ESA). The  $^{14}\text{C}^+$  ions are energy analyzed and focused in the ESA, detected and counted by a silicon surface barrier particle detector using total energy deposition per ion to set the measurement gate. Molecular isobars at  $m/z$  14, such as  $^{13}\text{CH}^-$  and  $^{12}\text{CH}_2^-$ , are the most abundant mass 14 ions and also pass through the injection magnet but dissociate in the electron stripper within the accelerator.  $^{14}\text{N}^-$  ions decay on a femtosecond time-scale and do not interfere with the analysis.

The normalized  $^{14}\text{C}$  concentrations are easily converted into moles of  $^{14}\text{C}$  per gram of carbon, becquerels (Bq) per gram of carbon or any other convenient unit. Since AMS was first applied to  $^{14}\text{C}$  dating, the Modern unit is often used. One Modern is defined as the radiocarbon activity of a sample of 1950 AD wood growing in the northern hemisphere, 13.56 dpm per gram of carbon, which is equivalent to  $6.11$  fCi  $\text{mg}^{-1}$  or  $97.8$  amol  $^{14}\text{C}$   $\text{mg}^{-1}$  carbon. This is the atmospheric  $^{14}\text{C}$  concentration due to cosmic radiation. Since the mid-19th century, two anthropogenic sources have significantly changed the atmospheric  $^{14}\text{C}$  levels: the burning of fossil fuels (decreasing the  $^{14}\text{C}$  concentration) followed by atmospheric nuclear weapons tests, doubling the concentration of  $^{14}\text{C}$  in the atmosphere by 1963. This excess  $^{14}\text{C}$  continues to dissipate into the oceans with a half-life of 15 years, and the current atmosphere has a  $^{14}\text{C}$  concentration of 1.04 Modern. This rapid increase and subsequent dissipation of atmospheric  $^{14}\text{C}$ , known as the 'bomb pulse' (Fig. 2), can be used to measure age or molecular turnover rates on the time-scale of years or decades in organisms that have lived after the 1960s.<sup>17–19</sup> This is of particular interest in neuroscience since turnover rates in the human brain and deposition rates of pathological structures extend to these time-scales,<sup>20,21</sup> or the lifetime of the organism. The use of  $^{14}\text{C}$  to determine the age of biological samples assumes that an organism's biosynthesis is in isotopic equilibrium with its carbon source(s).<sup>22–24</sup> Since the  $^{14}\text{C}$  concentration intercepts the bomb curve at least twice, dates derived by this method are ambiguous and resolving this ambiguity requires additional information.

Specific binding to or concentrations of  $^{14}\text{C}$ -labeled molecules in isolated neurological components require quantitation of the unlabeled molecular interaction partner

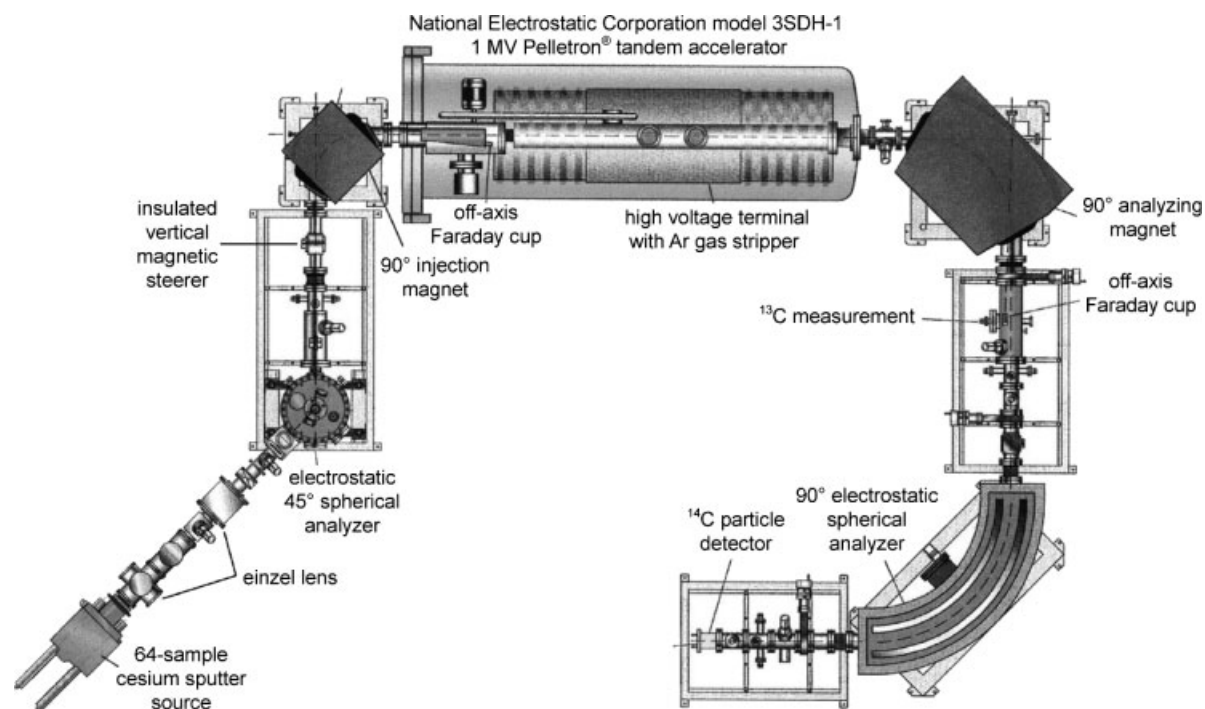


**Figure 1.** Schematic drawing of the National Electrostatic Corporation model 3SDH-1 1 MV Pelletron® tandem accelerator dedicated to biomedical analyses of  $^3\text{H}$  and  $^{14}\text{C}$  at the center for accelerator mass spectrometry and part of the NIH national research resource for biomedical AMS.

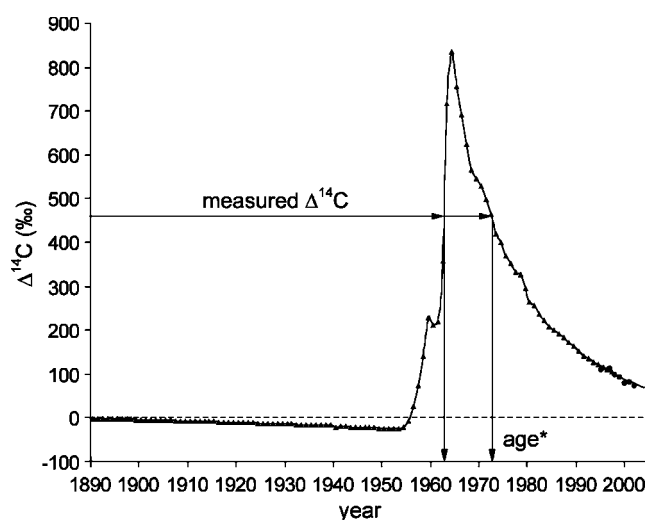


**Figure 2.** Atmospheric nuclear weapons tests in the 1950s and 1960s added significant amounts of  $^{14}\text{C}$  to the environment. This 'bomb curve' can be used for dating recent biological material. Superimposed on the bomb spike is the addition of  $^{14}\text{C}$ -depleted  $\text{CO}_2$  from burning fossil fuels. Data from the northern hemisphere: Black Forest (triangles)<sup>54</sup> and Sweden (circles) (B. A. Buchholz *et al.*, unpublished data). The  $\Delta^{14}\text{C}$  is the deviation from the Modern standard (see above). \*The age of the biological material is calculated assuming the organism's biosynthesis is in isotopic equilibrium with its carbon sources. Choosing between the two dates requires additional data.

(e.g. a protein) or the amount of carbon in the sample. We recently introduced a general method based on ion energy loss for this purpose.<sup>25</sup> This method based on a commercially available alpha spectrometer has a lower sample mass limit of  $\sim 100$  ng and, unlike spectrophotometric methods, it is independent of the functional groups on the quantified isolate. This technique permits quantitative isotope dilution for the very small samples often incurred in neurological dissections.

## INSECTICIDES AND BLOOD–BRAIN BARRIER PERMEABILITY

Organophosphates, such as diisopropyl fluorophosphate (DFP), are frequently used as insecticides. DFP has previously been used as an experimental agent in neuroscience for its ability to inhibit cholinesterases and induce delayed peripheral neuropathy<sup>26</sup> and as an ophthalmic cholinesterase inhibitor in glaucoma treatment.<sup>27,28</sup> Accidental exposure can have severe acute and chronic consequences.<sup>29,30</sup> There are also reported chronic effects from repeated low-dose exposure.<sup>31,32</sup> The sensitivity of AMS permits the study of low-level (sub-toxic) exposure to acutely toxic compounds *in vivo* (DFP has an oral  $\text{LD}_{50}$  in rat of  $1.3 \text{ mg kg}^{-1}$ ).

The effect on the permeability of the blood–brain barrier (BBB) to low doses of pesticide mixtures was investigated using [ $^{14}\text{C}$ ]DFP as a quantifiable probe of effects due to unlabeled parathion (PTN), permethrin (PER) and pyridostigmine bromide (PYB) separately and in conjunction.<sup>33</sup> CD2/F1 male mice received  $1 \mu\text{g kg}^{-1}$  PTN,

PER, PTN + PER or blank carrier all with and without  $50 \mu\text{g kg}^{-1}$  PYB in moist food through a 5-day fast/feed cycle. On day 6, four mice per group received  $1 \mu\text{g kg}^{-1}$  [ $^{14}\text{C}$ ]DFP (2 nCi  $^{14}\text{C}$ ) in moist food. Dry food and water were then available *ad libitum* for 48 h and mice were killed by  $\text{CO}_2$  asphyxiation according to AAALAC guidelines.<sup>34</sup> Blood, skeletal muscle, liver, spleen and brain were harvested and  $^{14}\text{C}$  contents measured by AMS. Soluble [ $^{14}\text{C}$ ]DFP was removed from the left hemisphere of each mouse brain using a series of cell disruptions, washes and centrifugations. PYB showed an overall protective effect against tracer binding in plasma, red blood cells, muscle and brain that is not explained by competitive binding, owing to the low concentrations used. The protective nature of PYB in the brain did not fit a dose-dependent extrapolation from higher dose studies.<sup>35</sup> Induction of a protective esterase activity in another tissue that lowered plasma DFP, and consequently brain DFP, is consistent with our observations, as is decreased DFP bioavailability due to increased intestinal peristalsis. The induced enzyme had to be specific to DFP and not affect PTN and PER, however, since pre-exposure to these increased DFP binding. Both PTN and PER induced a 25–30% increase in the amount of tracer reaching the brain with or without PYB. Overall binding of DFP in brain tissue increased with pre-exposure to PTN and PER and decreased with pre-exposure to PYB. Individual protein binding was not pursued in the original study. Proteins in brain tissue and plasma from DFP-treated mice have subsequently been separated with SDS–PAGE and IEF (Fig. 3). The increase in brain-bound DFP observed at 48 h could be due to either increased absorption of DFP or greater retention. Most of the dose DFP was excreted in urine within 48 h, and we did not observe changes in levels of DFP in other tissues to balance the changes in the brain. The oral doses of the pesticides used in the study were similar to those found in foods, drinking of surface waters or home pesticide use. If the increase in brain DFP level is due to increased permeability of the BBB, other toxins or pathogens might also induce increased BBB permeability with low pesticide exposure. The high sensitivity of AMS allowed the probing of specific biochemical pathways using physiological doses, which did not perturb the natural system of the model animal.

We showed that identification of the target enzyme or receptor is amenable to common protein separation and identification methods, such as gel electrophoresis and mass spectrometry.<sup>11,36,37</sup> Uniform gel slices from IEF or SDS–PAGE are dried and combusted for AMS analysis, superimposing  $^{14}\text{C}$  traces on the separated proteins.<sup>11,36</sup> Fig. 3 illustrates the use of standard proteomic techniques to assist the identification of binding partners, in this case DFP in mouse plasma. The intensity in the 'virtual gels' is the  $^{14}\text{C}$  count from AMS. The gel itself provides the carbon carrier. If the quantity of the protein is known or can be measured, the specific binding of the  $^{14}\text{C}$ -labeled molecule can be determined.

After the emergence of Gulf War Syndrome in veterans of the 1991 Gulf War, synergistic exposures to combinations of esterase inhibitors were a hypothesized contributor. We

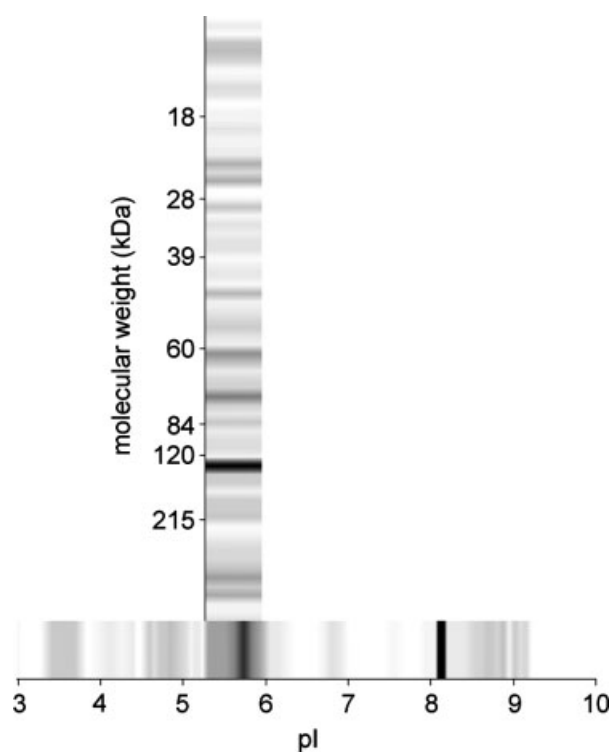


**Figure 3.** Measurements of adsorption and distribution of  $^{14}\text{C}$ -labeled drugs or toxins and identification of target protein(s) are compatible with established methods in proteomics, such as gel electrophoresis. Shown here are two 'virtual gel' [ $^{14}\text{C}$ ]DFP traces in isoelectric focusing (IEF) and subsequent sodium dodecyl sulfate polyacrylamide gel electrophoresis (SDS-PAGE) of the pI range 5.2–5.9 in the same mouse plasma. The molecular masses of the major bands in this pI range are consistent with monomers and dimers of esterase 1 (carboxylesterase) (61 kDa), butyrylcholinesterase (69 kDa) and paraoxonase (K-45) (45 kDa). (Human) butyrylcholinesterase has been shown to display a smear from pI 4 to 5.7 in IEF<sup>55</sup> and esterase 1 and paraoxonase are both predicted to be within the selected pI range. These proteins are all known to bind strongly organophosphates such as DFP. If sufficiently abundant, the proteins could be identified by in-gel enzymatic digestion, mass spectrometry and peptide mass fingerprinting. Definitive identifications may require further separation. The total  $^{14}\text{C}$  levels in these bands are in the low attomole range.

used AMS to examine the effect of chronic exposure to PYB ( $7.75 \text{ mg kg}^{-1} \text{ day}^{-1}$  in chow) on acute doses of  $^{14}\text{C}$  labeled PER ( $4.75 \mu\text{g kg}^{-1}$  i.p.). At 1 h after dosing, the amount of PER in brain and spinal cord was reduced by 30% for animals receiving PYB. At 24 h, there was no difference in PER in the brain but the spinal cord had 70% less PER with PYB exposure. The levels of PER in the plasma was the same for each dose group.<sup>38</sup> The sensitivity of the measurement was  $\text{pg g}^{-1}$  PER equivalents in dissected tissue. Since PER and PYB are not direct competitors for enzyme binding, and the quantified effect is too large for competitive inhibition at these doses, a physiological effect such as decreased bioavailability is again suggested.

## TURNOVER, ALZHEIMER'S DISEASE AND CARBON-14 DATING ON THE BOMB CURVE

It is estimated that more than 90% of degenerative dementias are proteinopathies, i.e. caused by abnormal protein aggregation.<sup>39</sup> In Alzheimer's disease (AD), these are primarily different amyloid beta ( $A\beta$ ) peptides and a hyperphosphorylated form of the tau protein,<sup>40</sup> whereas alpha-synuclein is implicated in Parkinson's disease, dementia with Lewi bodies and other forms of dementia.<sup>41,42</sup> Although numerous contributing factors have been identified, the etiology of these diseases is generally poorly understood.

The bomb pulse of  $^{14}\text{C}$  (Fig. 2) was used to determine the average date of formation of the major histopathological features in Alzheimer's disease (AD) brain: extracellular senile plaques (SP), composed primarily of amyloid beta peptide, and intracellular neurofibrillary tangles (NFT), composed of paired helical filaments containing hyperphosphorylated tau protein. Both are filamentous and essentially insoluble proteins.<sup>40</sup> The changing  $^{14}\text{C}$  level of contemporary carbon was also used to determine the carbon 'age' of normal brain tissue (1.4 years). The SP and NFT structures have a much slower carbon turnover rate than normal tissue and are not in a formation/degradation equilibrium. Bulk tissue samples used for isolation of NFT and SP fractions consisted of single cerebral hemispheres from which most of the occipital cortex, basal ganglia and thalamus were removed. The samples were taken at autopsy from six AD subjects from 1994 to 1998. A detailed description of the isolation procedure is available elsewhere.<sup>43</sup> Isolated SP and NFT were oxidized to  $\text{CO}_2$  and reduced to graphite using the high-precision individual reactor method employed for radiocarbon dating, so that samples containing as little as  $20 \mu\text{g}$  of carbon could be measured<sup>44</sup> (all other samples discussed herein were sufficiently large to be processed by the high-throughput method described by Ognibene *et al.*<sup>10</sup>).

The average age of isolated SP and NFT was significantly greater than normal tissue from the same subjects (SP by  $9.8 \pm 4.9$  years and NFT by  $9.4 \pm 3.8$  years). A clear and consistent pattern of formation of NFT and SP could not be formulated from this small number of analyzed subjects, but in four out of six cases, average SP or NFT or both predated the onset of symptoms by as long as 9 years. Some samples produced an insufficient amount of carbon for successful measurement by AMS. We expect that more efficient isolation techniques that can accommodate smaller specimens from specific brain regions will produce more consistent patterns of formation. Such studies could provide valuable information on the etiology and progression of AD and other neurodegenerative proteinopathies.

## CONCLUSIONS AND FUTURE OUTLOOK

AMS is a proven sensitive and robust method for quantifying rare isotopes in biological systems. It is currently expanding into early pharmacokinetic studies in humans using microgram doses.<sup>3</sup> It is applicable to the study of blood-brain barrier transport of minute quantities of labeled compounds. While  $^{14}\text{C}$  AMS is extremely versatile, AMS also

provides exquisite sensitivity for other rare isotopes. Aluminum uptake and transport across the blood–brain barrier has been investigated using  $^{26}\text{Al}$  AMS and microdialysis.<sup>45,46</sup> Calcium, its concentration, spatial localization and dynamics are important in many neuronal processes, such as signaling, long-term potentiation and depression,<sup>47,48</sup> dendrite<sup>49</sup> and spine formation.<sup>50</sup> Although very sensitive fluorescent methods for quantifying  $[\text{Ca}^{2+}]$  *in vivo* and in real time are well established,<sup>51,52</sup> they require careful calibration and cannot *directly* distinguish between different sources of  $\text{Ca}^{2+}$ . Furthermore, the  $\text{Ca}^{2+}$ -sensitive dyes add a significant exogenous buffer capacity and distort the amplitude, time course and spread of  $[\text{Ca}^{2+}]$  signals.<sup>51</sup> High-throughput calcium-41 measurement by AMS have recently been demonstrated by Hillemonds *et al.*<sup>53</sup> The routinely achievable limit of quantitation in these measurements is 10 amol of  $^{41}\text{Ca}$ . Although this method cannot compete at present with the sensitivity or the spatial and temporal resolution of fluorescence methods, it may be applicable as an absolute reference for the fluorescent dyes and for labeling a specific pool or pulse of calcium during an experiment. Since  $^{41}\text{Ca}$  can be quantitated at  $^{41}\text{Ca}/^{40}\text{Ca}$  isotope ratios down to  $10^{-13}$ ,<sup>53</sup> miniscule amounts of  $^{41}\text{Ca}$  could be measured in an abundance of stable calcium isotopes.

Given the present trend towards smaller,<sup>16</sup> less expensive and integrated AMS systems for carbon-14 and other isotopes, we believe that a technique as sensitive and versatile as AMS will have increasing utility in neuroscience and other biomedical disciplines.

### Acknowledgements

The authors thank Per Jesper Sjöström for valuable comments on the manuscript and Kurt W. Haack for AMS sample preparation. This work was partially supported by LLNL LDRD 01-ERI-006. The work was performed in part under the auspices of the US Department of Energy by the University of California Lawrence Livermore National Laboratory under Contract No. W-7405-ENG-48.

### REFERENCES

- Adelstein SJ, Manning FJ. *Isotopes for Medicine and the Life Sciences*. National Academy Press, Washington, DC: 1995.
- Dalvie D. Recent advances in the applications of radioisotopes in drug metabolism, toxicology and pharmacokinetics. *Curr. Pharm. Des.* 2000; **6**: 1009.
- Turteltaub KW, Vogel JS. Bioanalytical applications of accelerator mass spectrometry for pharmaceutical research. *Curr. Pharm. Des.* 2000; **6**: 991.
- Ognibene TJ, Amer H, Benjamin KR, Bench G, Vogel JS, Colvin ME. A protocol for the quantitative determination of biomolecules in individual cells. In preparation.
- Gilman SD, Gee SJ, Hammock BD, Vogel JS, Haack K, Buchholz BA, Freeman SPHT, Wester RC, Hui XY, Maibach HI. Analytical performance of accelerator mass spectrometry and liquid scintillation counting for detection of C-14-labeled atrazine metabolites in human urine. *Anal. Chem.* 1998; **70**: 3463.
- Vogel JS, McAninch J, Freeman SPHT. Elements in biological AMS. *Nucl. Instrum. Methods Phys. Res. B* 1997; **123**: 241.
- Yokel RA, McNamara PJ. Aluminium toxicokinetics: an updated minireview. *Pharmacol. Toxicol.* 2001; **88**: 159.
- Vogel JS, Southon JR, Nelson DE, Brown TA. Performance of catalytically condensed carbon for use in accelerator mass spectrometry. *Nucl. Instrum. Methods Phys. Res. B* 1984; **233**: 289.
- Vogel JS. Rapid Production of graphite without contamination for biomedical AMS. *Radiocarbon* 1992; **34**: 344.
- Ognibene TJ, Bench G, Vogel JS, Peaslee GF, Murov S. A high-throughput method for the conversion of  $\text{CO}_2$  obtained from biochemical samples to graphite in septa-sealed vials for quantification of C-14 via accelerator mass spectrometry. *Anal. Chem.* 2003; **75**: 2192.
- Vogel JS, Grant PG, Buchholz BA, Dingley K, Turteltaub KW. Attomole quantitation of protein separations with accelerator mass spectrometry. *Electrophoresis* 2001; **22**: 2037.
- Buchholz BA, Fultz E, Haack KW, Vogel JS, Gilman SD, Gee SJ, Hammock BD, Hui X, Wester RC, Maibach HI. HPLC-accelerator MS measurement of atrazine metabolites in human urine after dermal exposure. *Anal. Chem.* 1999; **71**: 3519.
- Shan G, Huang W, Gee SJ, Buchholz BA, Vogel JS, Hammock BD. Isotope-labeled immunoassays without radiation waste. *Proc. Natl. Acad. Sci. USA* 2000; **97**: 2445.
- Steen H, Pandey A. Proteomics goes quantitative: measuring protein abundance. *Trends Biotechnol.* 2002; **20**: 361.
- Lill J. Proteomic tools for quantitation by mass spectrometry. *Mass Spectrom Rev.* 2003; **22**: 182.
- Ognibene TJ, Bench G, Brown TA, Peaslee GF, Vogel JS. A new accelerator mass spectrometry system for C-14-quantification of biochemical samples. *Int. J. Mass Spectrom.* 2002; **218**: 255.
- Nydal R, Lövsæth K. Distribution of radiocarbon from nuclear tests. *Nature* 1971; **232**: 418.
- Levin I, Kromer B, Schochfischer H, Bruns M, Munnich M, Berdau D, Vogel JC, Munnich KO. 25 years of tropospheric C-14 observations in central Europe. *Radiocarbon* 1985; **27**: 1.
- Levin I, Böisinger R, Bonani G, Francey RJ, Kromer B, Munnich KO, Suter M, Trivett NBA, Wölfli W. In *Radiocarbon after Four Decades: an Interdisciplinary Perspective*, RE Taylor, A Long, RS Kra. (eds). Springer: New York, 1992; 503.
- Druffel EM, Mok HYI. Time history of human gallstones—application of the post-bomb radiocarbon signal. *Radiocarbon* 1983; **25**: 629.
- Mok HYI, Druffel ERM, Rampone WM. Chronology of cholelithiasis—dating gallstones from atmospheric radiocarbon produced by nuclear bomb explosions. *N. Engl. J. Med.* 1986; **314**: 1075.
- Broecker WS, Schulert A, Olson EA. Bomb  $^{14}\text{C}$  in human beings. *Science* 1959; **130**: 331.
- Harkness DD, Walton A. Further investigations of the transfer of bomb  $^{14}\text{C}$  to man. *Nature* 1972; **240**: 302.
- Stenhouse MJ, Baxter MS. Bomb C-14 as a biological tracer. *Nature* 1977; **267**: 828.
- Grant PG, Palmblad M, Murov S, Hillemonds DJ, Ueda DL, Vogel JS, Bench G. Alpha-particle energy loss measurement of microgram depositions of biomolecules. *Anal. Chem.* 2003; **75**: 4519.
- Lowndes HE, Baker T, Riker WF Jr. Motor nerve terminal response to edrophonium in delayed DFP neuropathy. *Eur. J. Pharmacol.* 1975; **30**: 69.
- Ferrer O. Clinical evaluation of DFP (diisopropyl fluorophosphate) in glaucoma. *Arch. Hosp. Univ.* 1950; **2**: 675.
- Holland MG. Autonomic drugs in ophthalmology: some problems and promises. I. Directly and indirectly acting parasymphathomimetic drugs. *Ann. Ophthalmol.* 1974; **6**: 447.
- Rosenstock L, Keifer M, Daniell WE, McConnell R, Claypoole K. Chronic central nervous system effects of acute organophosphate pesticide intoxication. The Pesticide Health Effects Study Group. *Lancet* 1991; **338**: 223.
- Senanayake N, Karalliedde L. Neurotoxic effects of organophosphorus insecticides. An intermediate syndrome. *N. Engl. J. Med.* 1987; **316**: 761.
- Prendergast MA, Terry AV Jr, Buccafusco JJ. Effects of chronic, low-level organophosphate exposure on delayed recall, discrimination, and spatial learning in monkeys and rats. *Neurotoxicol. Teratol.* 1998; **20**: 115.

32. Stone JD, Terry AV Jr, Pauly JR, Prendergast MA, Buccafusco JJ. Protractive effects of chronic treatment with an acutely sub-toxic regimen of diisopropylfluorophosphate on the expression of cholinergic receptor densities in rats. *Brain Res.* 2000; **882**: 9.
33. Vogel JS, Keating GA II, Buchholz BA. Protein binding of isofluorophate *in vivo* after coexposure to multiple chemicals. *Environ. Health Perspect.* 2002; **110**(Suppl 6): 1031.
34. AAALAC guideline. <http://www.aaalac.org/guide.htm>.
35. Abou-Donia MB, Goldstein LB, Jones KH, Abdel-Rahman AA, Damodaran TV, Dechkovskaia AM, Bullman SL, Amir BE, Khan WA. Locomotor and sensorimotor performance deficit in rats following exposure to pyridostigmine bromide, DEET, and permethrin, alone and in combination. *Toxicol. Sci.* 2001; **60**: 305.
36. Vogel JS, Hillegonds DJ, Palmblad M, Grant PG, Bench G. In *Methods in Proteome and Protein Analysis*, Kamp RM, Calvete JJ, Choli-Papadopolou. (eds). Springer: Heidelberg, 2004; 203.
37. Hillegonds DJ, Palmblad M, Grant PG, Bench G, Buchholz BA, Keating G, Vogel JS. In *Synthesis and Applications of Isotopically Labeled Compounds*, Dean DC, Filer CN, McCarthy KE. (ed.). Wiley: New York, 2004.
38. Buchholz BA, Pawley NH, Vogel JS, Mauthe RJ. Pyrethroid decrease in central nervous system from nerve agent pretreatment. *J. Appl. Toxicol.* 1997; **17**: 231.
39. Cummings JL. Toward a molecular neuropsychiatry of neurodegenerative diseases. *Ann. Neurol.* 2003; **54**: 147.
40. Selkoe DJ, Lansbury PT. In *Basic Neurochemistry: Molecular, Cellular and Medical Aspects*, GJ Siegel, BW Agravoff, RG Albers, SK Fisher, MD Uhler. (eds). Lippincott Williams and Wilkins: Philadelphia, 1999; 950–964.
41. Jellinger KA. Neuropathological spectrum of synucleinopathies. *Mov. Disord.* 2003; **18**(Suppl. 6): S2.
42. McKeith I, Mintzer J, Aarsland D, Burn D, Chiu H, Cohen-Mansfield J, Dickson D, Dubois B, Duda JE, Feldman H, Gauthier S, Halliday G, Lawlor B, Lippa C, Lopez OL, Carlos Machado J, O'Brien J, Playfer J, Reid W. Dementia with Lewy bodies. *Lancet Neurol.* 2004; **3**: 19.
43. Lovell MA, Robertson JD, Buchholz BA, Xie C, Markesbery WR. Use of bomb pulse carbon-14 to age senile plaques and neurofibrillary tangles in Alzheimer's disease. *Neurobiol. Aging* 2002; **23**: 179.
44. Vogel JS, Southon JR, Nelson DE. *Nucl. Instrum. Methods Phys. Res. B* 1987; **29**: 50.
45. Yokel RA, Rhineheimer SS, Sharma P, Elmore D, McNamara PJ. Entry, half-life, and desferrioxamine-accelerated clearance of brain aluminum after a single (26)Al exposure. *Toxicol. Sci.* 2001; **64**: 77.
46. Yokel RA. Brain uptake, retention, and efflux of aluminum and manganese. *Environ. Health Perspect.* 2002; **110**(Suppl. 5): 699.
47. Zucker RS. Calcium- and activity-dependent synaptic plasticity. *Curr. Opin. Neurobiol.* 1999; **9**: 305.
48. Sjöström PJ, Nelson SB. Spike timing, calcium signals and synaptic plasticity. *Curr. Opin. Neurobiol.* 2002; **12**: 305.
49. Sin WC, Haas K, Ruthazer ES, Cline HT. Dendrite growth increased by visual activity requires NMDA receptor and Rho GTPases. *Nature* 2002; **419**: 475.
50. Maletic-Savatic M, Malinow R, Svoboda K. Rapid dendritic morphogenesis in CA1 hippocampal dendrites induced by synaptic activity. *Science* 1999; **283**: 1923.
51. Sabatini BL, Maravall M, Svoboda K. Ca(2+) signaling in dendritic spines. *Curr. Opin. Neurobiol.* 2001; **11**: 349.
52. Yasuda R, Nimchinsky EA, Scheuss V, Pologruto TA, Oertner TG, Sabatini BL, Svoboda K. Imaging calcium concentration dynamics in small neuronal compartments. *Sci. STKE.* 2004; **2004**: 15.
53. Hillegonds DJ, Fitzgerald R, Herold D, Lin Y, Vogel JS. High throughput measurement of <sup>41</sup>Ca by accelerator mass spectrometry to quantitate small changes in individual human bone turnover rates. *J. Assoc. Lab. Autom.* 2004; **9**: 99.
54. Levin I, Kromer B. Twenty years of atmospheric (CO<sub>2</sub>)-C-14 observations at Schauinsland station, Germany. *Radiocarbon* 1997; **39**: 205.
55. Nachon F, Nicolet Y, Viguie N, Masson P, Fontecilla-Camps JC, Lockridge O. Engineering of a monomeric and low-glycosylated form of human butyrylcholinesterase—expression, purification, characterization and crystallization. *Eur. J. Biochem.* 2002; **269**: 630.